Marine Mammal Science

MARINE MAMMAL SCIENCE, 34(2): 347–364 (April 2018)

DOI: 10.1111/mms.12476

Age estimation in bowhead whales using tympanic bulla histology and baleen isotopes

JENNIFER D. SENSOR,[1,2] Department of Anatomy and Neurobiology, Northeast Ohio Medical University, Rootstown, Ohio 44240, U.S.A; **JOHN C. GEORGE,** Department of Wildlife Management, North Slope Borough, Barrow, Alaska 99723, U.S.A; **MARK T. CLEMENTZ,** Department of Geology and Geophysics, University of Wyoming, Laramie, Wyoming 82071, U.S.A; **DENISE M. LOVANO** and **DAVID A. WAUGH,** Department of Anatomy and Neurobiology, Northeast Ohio Medical University, Rootstown, Ohio 44240, U.S.A; **GEOF H. GIVENS,** Givens Statistical Solutions LLC, 4913 Hinsdale Drive, Fort Collins, Colorado 80526, U.S.A; **ROBERT SUYDAM** and **RAPHAELA STIMMELMAYR,** Department of Wildlife Management, North Slope Borough, Barrow, Alaska 99723, U.S.A; **J. G. M. THEWISSEN,** Department of Anatomy and Neurobiology, Northeast Ohio Medical University, Rootstown, Ohio 44240, U.S.A.

ABSTRACT

Tympanic bullae and baleen plates from bowhead whales of the Western Arctic population were examined. Growth layer groups (GLGs) in the involucrum of the tympanic bone were used to estimate age of the whales, and compared to stable isotope signatures along transects of baleen plates and the involucrum. The involucrum of the tympanic bone consists of three regions that form *in utero*, during nursing in the first year, and during the first decades of life, respectively. Life history events, such as annual migration, are recorded in the bowhead tympanic bulla. It is likely that bone growth in the bowhead tympanic occurs during periods of high food intake, while slow or arrested growth occurs during periods of low food intake. Comparisons between numbers of GLGs in the tympanic, number of isotopic oscillations in a baleen plate, length of the baleen plate, and total whale length show correlation coefficients as high as 0.97. The tympanic GLG method is particularly useful for estimating the age of whales up to 20 yr old.

Key words: Balaena, tympanic bulla, GLGs, LAGs, Arctic, stable isotopes.

Estimating the age of individual bowhead whales (*Balaena mysticetus*) is important in the management of existing populations. Several age estimation methods are available, but only cover limited parts of the bowhead lifespan. Growth models utilize baleen length (Lubetkin *et al*. 2008, 2012), isotope oscillations within baleen plates (Schell *et al*. 1989*a*, Schell and Saupe 1993), numbers of corpora albicantia in sexually mature females (George *et al*. 2011, Tarpley *et al*. 2016), and enantiomer ratios in the alpha-crystalline of the eye lens (George *et al*. 1999, Rosa *et al*. 2004).

[1]Corresponding author (e-mail: jennifer.sensor@gmail.com).
[2]Current address: Department of Physical Therapy, University of Mount Union, Alliance, Ohio 44601, U.S.A.

A critical age range for which most of these methods are imprecise or inadequate is between 10 and 30 yr.

Whereas growth layer groups (GLGs) in the dentin of odontocete teeth are often easily readable for age estimation (Perrin and Myrick 1980, Hohn 2009), this is not usually the case for GLGs in the bones of whales (Larsen and Kapel 1982, 1983; Olsen 2002; Olsen *et al*. 2003). One exception to this may be the tympanic bullae of baleen whales (Klevezal and Mitchell 1971; Christensen 1981, 1995; Sukhovskaya *et al*. 1985; Klevezal *et al*. 1986; Konrádsson and Sigurjónsson 1989; Klevezal 1996; Hohn 2009). Similarly, Marmontel *et al*. (1996) used histology of the periotic bone of manatees (*Trichechus manatus*) to estimate age. These authors showed that the number of periotic GLGs correlates well with the age of the animal, with the best accuracy for manatees up to 10–15 yr of age.

Here, we investigate the microstructure of the involucrum part of the tympanic bone in a sample of the Western Arctic population of bowhead whales. We focus on GLGs, as defined by Perrin and Myrick (1980) for marine mammals, in the periosteal region of tympanic bullae and assess their potential to estimate age. In addition to "GLG" we also use two other terms defined by Perrin and Myrick (1980). "Incremental growth layer" is defined as a "discernible layer occurring parallel to the formative surface of a hard tissue (dentine, cementum, bone) which shows any contrast with adjacent layers" (p. 49). "Accessory layers" are defined as "any single layered component of a GLG which is discernible from adjacent layers in a hard tissue" (p. 48). We also occasionally use bone histological terms defined by Huttenlocker *et al*. (2013) as they are used in the broader field of hard tissue histology (see also Francillon-Vieillot *et al*. 1990, de Ricqlès *et al*. 1991, Currey 2003).

We characterize the different parts of the involucrum histologically and isotopically, and compare these results with data on baleen plate length and number of isotopic oscillations in the baleen.

In the Western Arctic population, baleen stable isotope values record the fall migration of the whales from the Beaufort Sea to the Chukchi and eventually the Bering Sea where they winter (Saupe *et al*. 1989; Schell *et al*. 1989*a, b*; Schell and Saupe 1993). Life history events, such as nursing and weaning are also recorded by stable isotopes. In addition, birth is recorded morphologically in the baleen, since the direction of plate growth changes. This produces a neonatal notch in the labial side of the baleen plate (Zenitani and Kato 2010).

Materials and Methods

Inupiat subsistence hunters in Barrow, Alaska, harvest a small number of bowhead whales during the annual migration in Spring and Fall (Suydam and George 2004). Data and samples were gathered by scientists from the Department of Wildlife Management of the North Slope Borough, Barrow, Alaska (NSB-DWM) under NOAA-NMFS permit # 17350-01. We studied tympanic bullae and the longest baleen plate. All specimens (baleen, sectioned slices of the involucrum, and thin sections of the involucrum) were subsequently deposited in the collections of the NSB-DWM.

We cut rostral and caudal slices in the coronal plane of the involucrum of the bulla with an approximate thickness of 3 mm. The involucrum and its periosteal region are thickest in the caudal slices, and this region is the focus of our study (Fig. 1A, B). For two specimens (2014B11, 2014B14) a simple bone core was taken from the caudal involucrum, and slices were prepared from it.

Bone slices were embedded in Buehler EpoThin epoxy resin, polished on one side, and mounted (polished side down) with either epoxy or Loctite 349 (a UV

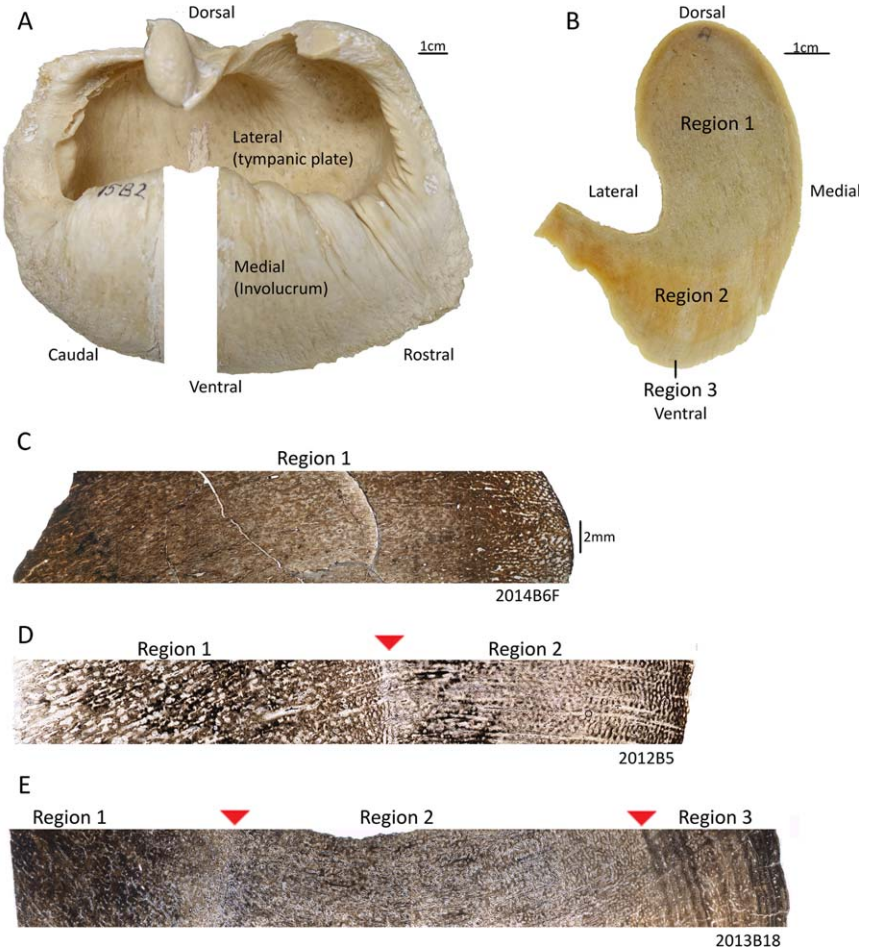

Figure 1. (A) Tympanic bulla of bowhead whale NSB-DWM 2015B2 with caudal involucrum slice removed. (B) Anterior view of involucrum slice taken from NSB-DWM 2015B2. (C) Microstructure of transect of involucrum from a fetal bowhead NSB-DWM 2014B6F, showing that only region 1 is present. (D) Microstructure of transect of involucrum from bowhead whale NSB-DWM 2012B5, showing regions 1 and 2. This animal is estimated to be 1 yr old based on baleen length and single baleen $\delta^{13}C$ oscillation. (E) Microstructure of transect of involucrum from bowhead whale NSB-DWM 2013B18 estimated to be about 10 yr of age using GLGs. Red arrowheads indicate borders of regions. Two mm scale bar refers to C–E.

curing adhesive). Slices were then ground down to approximately 50–100 μm thickness and polished. We used 2x and 4x objectives under brightfield lighting with an Olympus BX40 microscope to take photos.

We decalcified one bone slice for 1 wk in formic acid, embedded it in paraffin, and stained it with hematoxylin and eosin, following a method modified from Christensen (1981) and Marmontel *et al*. (1996). Although this method helped to distinguish GLGs close to the periosteal edge, deep GLGs became diffuse and unreadable.

For two bullae specimens (NSB-DWM 2012B5, 2013B6), samples were collected for $\delta^{13}C$ analysis of structural carbonate within the bone mineral (bioapatite). Approximately 6–9 mg of bone powder was drilled at 1 mm intervals along a transect starting at the center of the involucrum to the ventromedial edge. Since the incremental growth layers in the periosteal region are thin, collection of samples sufficiently large for isotopic analysis could not be accomplished for all GLGs. Bone samples were taken using Carpenter Microsystems 2 software with a 600 µm drill bit. Sample sites were 5–7 mm long and were 600–1,500 µm deep. Approximately 0.6 mg of bone powder from each sample was dissolved in 100% phosphoric acid at 25°C and the resulting CO_2 was analyzed. Stable isotope analysis of bone mineral employed a ThermoFisher GasBench II coupled to a continuous flow ThermoFisher Delta Plus XP Isotope Ratio Mass Spectrometer (IRMS). Repeated analysis of internal lab standards (NIST SRM 1486, NIST SRM 120c) and international standards established an instrument precision (1 σ) of $<0.1‰$ for $\delta^{13}C$ values.

Investigations of the stable isotopes of baleen, especially ^{13}C and ^{15}N, have been carried out by a number of authors (Schell *et al*. 1989*a, b*; Schell 1992; Withrow *et al*. 1992; Hobson and Schell 1998; Lee *et al*. 2005; Lubetkin *et al*. 2008; Matthews and Ferguson 2015*b*), and we adapted their methods. We determined baleen plate lengths and extracted powdered samples every centimeter from the most proximal end (embedded in the palate) to the most distal (protruding into the oral cavity), along the labial edge using a Foredom microdrill. Dry baleen powder samples were weighed in tin capsules (~1 mg) and combusted using a Costech 4010 Elemental Analyzer coupled to a continuous flow ThermoFisher Delta Plus XP IRMS. Instrument precision (1 σ) was determined as $<0.1‰$ for $\delta^{13}C$ and $\delta^{15}N$ values through repeated measurement of internal lab standards (acetanilide, glutamic acid, keratin) and international standards. All $\delta^{13}C$ and $\delta^{15}N$ isotope values are reported relative to Vienna Pee Dee Belemnite (VPDB) scale and AIR (Atmospheric nitrogen) scale, respectively, in standard delta notation: $\delta^{13}C$ or $\delta^{15}N\ (‰) = (R_{sample}/R_{standard} - 1)$ x 1,000 where R is the ratio $^{13}C/^{12}C$ or $^{15}N/^{14}N$ in a sample and standard (VPDB or AIR).

Counting the number of annual isotopic oscillations along a baleen plate with a neonatal notch provides a method of age estimation. In older animals that lack a neonatal notch, counting annual isotopic oscillations provides only a minimum age estimate, as part of the baleen has worn off.

Baleen plate length correlates well with age for certain age ranges of male and female bowheads (Lubetkin *et al*. 2008, 2012). Lubetkin *et al*. (2012) fit a sex-specific von Bertalanffy II growth model with a juvenile growth spurt which yielded the predictive model $A = c_0 + c_1 \ln[c_2/(c_3 - L)]$. Where A is age, L is the (longest) baleen plate length, and the estimated parameters (c_0–c_3) are given in Table 1. We estimated relationships between the number of GLGs and baleen length, estimated whale age, and number of stable $\delta^{13}C$ isotope cycles using simple linear regression. A log-log fit was used when appropriate to account for nonlinearity and/or to stabilize variance.

RESULTS

Tympanic Bone Structure

Three roughly concentric regions can be distinguished on a slice of the tympanic bulla, referred to as regions 1–3 (Fig. 1B–E). Region 1 covers most of the cross-sectional area. Region 2 is external to region 1 on all sides, and is thickest on the

Table 1. Estimated parameters for the von Bertalanffy II growth model of Lubetkin *et al.* (2012).

Parameter	Small bowhead longest plate ≤ 1.81 m	Large male bowhead longest plate > 1.81 m	Large female bowhead longest plate > 1.81 m
c_0	0	10	10
c_1	3.1075	26.4135	37.3516
c_2	166.56	136.5578	193.1078
c_3	187.82	317.71	374.26

ventromedial side of the involucrum. Region 3 is a narrow band along the periosteal surface, external to region 2. On the ventromedial side of the slice, the bulla forms a gnarled crest with many infoldings. In this area, region 3 is thicker than anywhere else and displays the best developed GLGs.

On the cut slice, region 1 is the darkest in color. On thin-section in coronal view, it consists primarily of woven bone with a largely reticular pattern of vasculature (fibrolamellar bone; Fig. 1C–E). Vessels are oriented predominantly dorso-medial in postnatal individuals (Fig. 1D,E). Primary osteons occur in region 1, and this region lacks Haversian systems proper, with no cement line or evidence of resorption around the osteons. Some specimens, in addition to their reticular vasculature, have radial vessels that cross the interface between regions 1 and 2 (NSB-DWM 2012B5, 2013B6, 13B15, 2014B11, 2014B14, and 2015B24). Additionally, specimen NSB-DWM 2015B2 has some radial vessels throughout region 1. Region 1 is the only region present in the tympanic bone of a fetus, and is spongy in appearance, being poorly mineralized (Fig. 1C; NSB-DWM 20146F).

On a cut slide, region 2 is white to yellow in color (Fig. 1B). It consists predominately of primary woven bone with reticular and radial vasculature (fibrolamellar bone). Most of the longer vessels extend parallel to each other and curve in a ventromedial direction, as opposed to the general dorso-medial direction of vessels in region 1. Primary osteons occur within region 2, but as in region 1, there is no evidence of remodeling.

Region 3 consists of incremental growth layers that constitute GLGs. These are subsequent dark and light/translucent layers (Fig. 2–7). Accessory layers, which are dissimilar from one GLG to another, may occur within a GLG (white boxes in Fig. 2, 3, 5, 6; NSB-DWM 2013B1, 2013B6, 2013B18, 2014B14, 2015B16, and 2015B24) and are not cyclic.

The dark incremental growth layers of a GLG are thicker than the translucent growth layers, except near the periosteal surface in some older individuals, when total GLG thickness decreases. Histologically, growth layers may consist of slow growing lamellar bone (Fig. 2, 4, 6; NSB-DWM 2011B9, 2013B5, 2014B11, 2014B14, 2015B16, 2015B17, 2015B19, and 2015B24), woven bone with reticular vasculature (Fig. 2, 3; NSB-DWM 2013B15 and 2013B18) or a combination of the two (Fig. 2, 6; NSB-DWM 2013B6 and 2015B2).

Radial and longitudinal vessels can occur in region 3, and these intersect with the GLGs at a variety of angles. Some specimens display only radial vessels (Fig. 2, 3; NSB-DWM 2013B5, 2013B6, and 2013B18) in the dorsal portion of a tympanic slice, while others display both types of vasculature (Fig. 4, 6; NSB-DWM 2011B9, 2014B11, 2014B14, 2015B2, 2015B16, 2015B17, and 2015B24). Small secondary

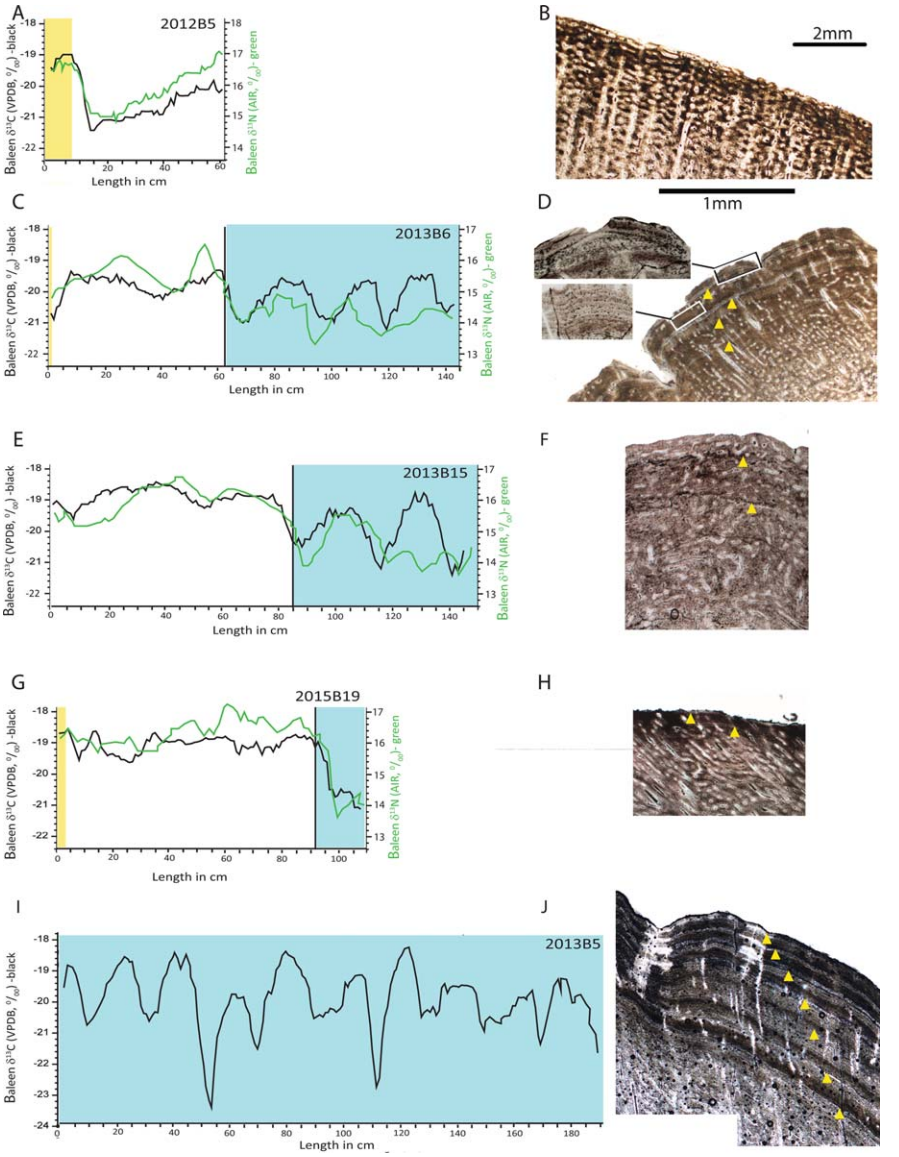

Figure 2. (A, C, E, G, I) δ^{13}C (black) and δ^{15}N (green) values from baleen keratin taken along the total length of the plate from distal (left) to proximal (right). Yellow zones within the plots indicate isotope values of prenatally formed baleen (as indicated by the neonatal notch), white indicates the nursing period, blue indicates postweaning period. (B, D, F, H, J) Details of regions 2 and 3 microstructure of tympanic bullae from A, C, E, G, I, respectively. Yellow arrowheads in histological images indicate boundaries between GLGs, 2 mm scale bar refers to all these images. Boxes in D refer to insets and show accessory layers, 1 mm scale bar refers to insets only (A, B) NSB-DWM 2012B5. (C, D) NSB-DWM 2013B6. (E, F) NSB-DWM 2013B15. (G, H), NSB-DWM 2013B19, NSB-DWM 2013B5.

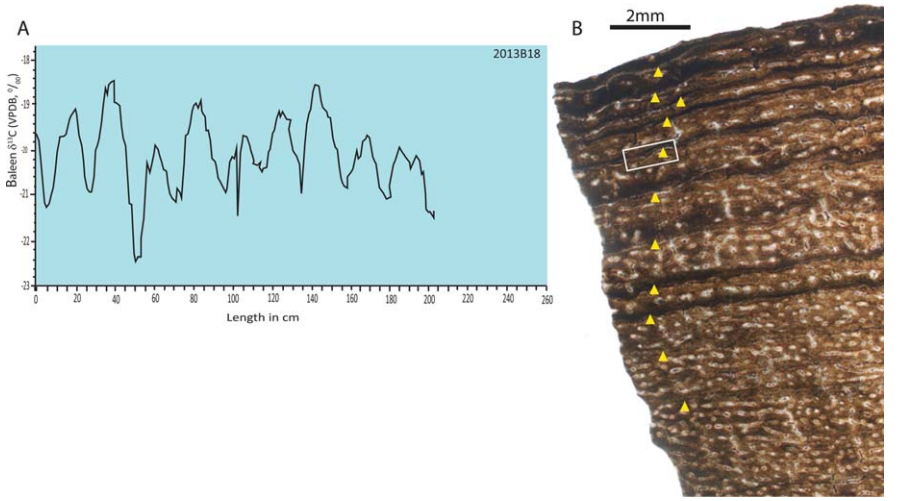

Figure 3. (A) δ^{13}C values of baleen keratin of whale NSB-DWM 2013B18 covering the entire length of the plate from distal (left) to proximal (right), this baleen only preserves a record of the independent feeding period. (B) Region 3 microstructure of tympanic bulla of the same whale. Yellow arrowheads indicate boundaries between GLGs. A white box indicates presence of accessory layers.

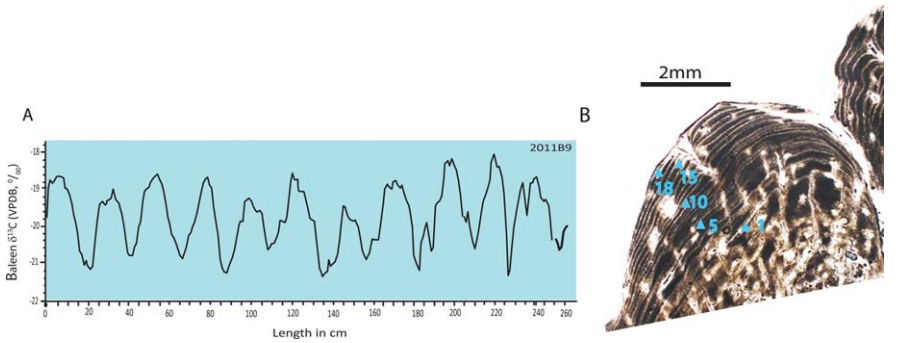

Figure 4. (A) δ^{13}C values from baleen keratin of whale NSB-DWM 2011B9 along the entire length of the plate from distal (left) to proximal (right), this baleen only preserves a record of the independent feeding period. (B) Region 3 microstructure of tympanic bullae of the same whale. Blue arrowheads mark the boundary of the first and last GLG as well as every 5th GLG.

osteons occur in some of the older whales (Fig. 7; NSB-DWM 2013B1, 2015B2, 2015B17, and 2015B24).

Stable Isotopes

Isotopic analyses show that baleen δ^{13}C and δ^{15}N values oscillate along the length of the plate (Fig. 2–5). The neonatal notch of the baleen plate is a morphological indicator of the timing of birth, and can be used to calibrate isotope

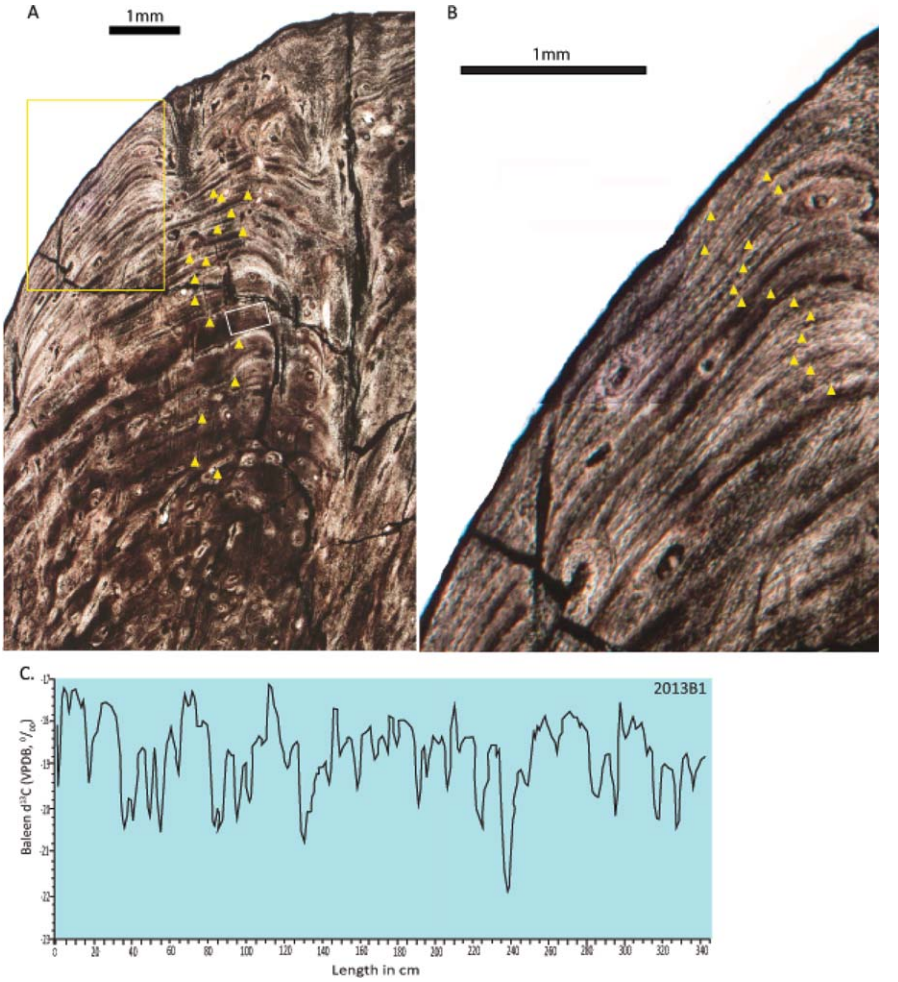

Figure 5. (A) Region 3 microstructure of the tympanic bone of whale NSB-DWM 2013B1. Yellow box is enlarged in B. (B) Enlarged view of GLGs magnified from A, yellow arrowheads indicate boundaries between GLGs, and white box marks area of accessory lines. (C) $\delta^{13}C$ values of baleen keratin along the entire length of the plate from distal (left) to proximal (right) of this whale.

signals around birth. Baleen growth in the first year (which includes the nursing period) is approximately 75 cm (George *et al*. 2016). In our specimens, at lengths between 62 and 92 cm we observed a drop in $\delta^{15}N$ values (Fig. 2), and this drop is statistically significant for different specimens (NSB-DWM 2013B15: white area of Fig. 2E: 1 $\sigma = 0.26‰$, blue area: 1 $\sigma = 0.69‰$, $F = 6.593$, $P < 0.0001$; NSB-DWM 2013B6: white area of Fig. 2B: 1 $\sigma = 0.25‰$; blue area: 1 $\sigma = 0.49‰$, $F = 3.844$, $P < 0.0001$). We also determined $\delta^{13}C$ composition for transects through region 1 and 2 of two involucra (Fig. 8), in order to compare these with baleen isotope signals and baleen morphology (neonatal notch).

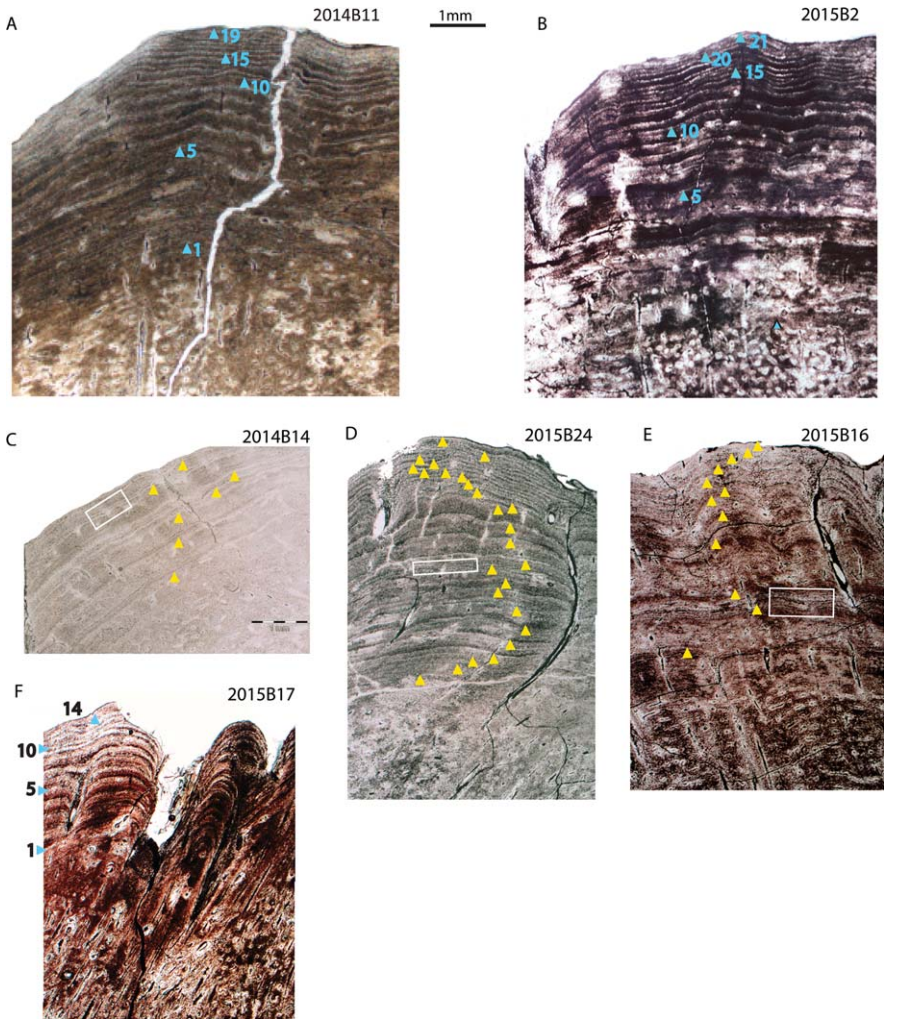

Figure 6. Region 3 microstructure of six tympanic bone slices under brightfield magnification. (A) NSB-DWM 2014B11. (B) NSB-DWM 2015B2. (C) NSB-DWM 2014B14. (D) NSB-DWM 2015B24. (E) NSB-DWM 2015B16. (F) NSB-DWM 2015B17. Yellow arrowheads indicate boundaries between GLGs, and blue arrowheads are placed on the boundary of the first and last GLG and every 5th GLG. A white box marks accessory lines.

Life History Data

Table 2 compiles biological data with age estimates for the individuals studied. Figure 9 explores regression models for these data. Figure 9A shows a linear regression of whale length on GLGs. The slope and intercepts are 0.264 (SE = 0.014) and 8.018 (SE = 0.207), respectively, with $R^2 = 0.97$. Figure 9B plots baleen plate length in a log-log regression on GLG number. Since baleen plate length does not grow linearly with whale age, we fitted these data to a nonlinear curve. The

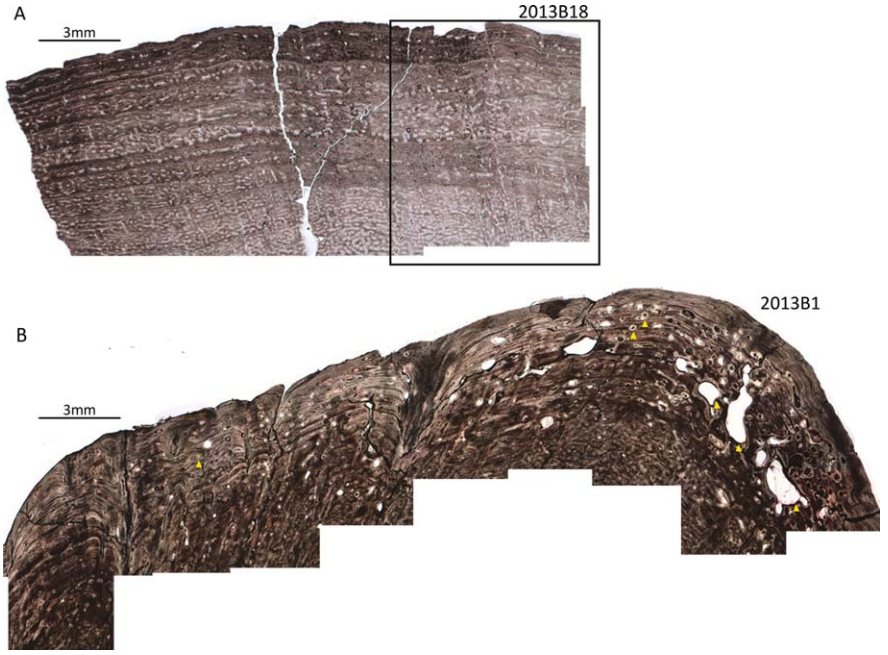

Figure 7. (A) Low magnification image of region 3 of the tympanic bone of NSB-DWM 2013B18. GLGs are distinctive on the left side of the image but less so on the right in the black box. (B) Low magnification image of region 3 in NSB-DWM 2013B1. Yellow arrows indicate presence of secondary osteons and areas of resorption.

relationship between estimated age (based on baleen length) and number of GLGs is essentially linear (Fig. 9C), but a log-log fit was required to equalize variance. The slope and intercept estimates for such a fit are 1.097 (SE = 0.074) and 0.168 (SE = 0.173) respectively, with $R^2 = 0.95$. Figure 9D shows a linear regression of the number of stable $\delta^{13}C$ cycles in baleen plate GLGs. The slope and intercept estimates are 0.659 (SE = 0.072) and 1.961 (SE = 1.059), respectively, with $R^2 = 0.94$. For each of these four models, we tested sex as a potential additional predictor, but this factor was not statistically significant in any model.

Discussion

The bone histology of regions 1–3 displays a pattern that indicates that bone growth in the bowhead tympanic is similar to that in other mammals (Huttenlocker *et al*. 2013, Woodward *et al*. 2013). Fibrolamellar bone, as found in region 1 and 2 indicates fast growth. This type of bone is also located in the cortex of long bones of land mammals, a region comparable to region 2 of the bowhead tympanic. In contrast, the periosteal surface of mammalian long bones is similar to region 3 of the bowhead tympanic and consists of slow-growing, parallel-fibered or lamellar bone. With age, bone remodels, but the rate for this process varies (Klevezal 1996). We see some evidence of remodeling in bowhead in the form of secondary osteons (NSB-DWM 2013B1, 2015B2, 2015B17, 2015B24; Fig. 5–7), but only in older individuals. Remodeling is also slow to occur in the periotics of manatees

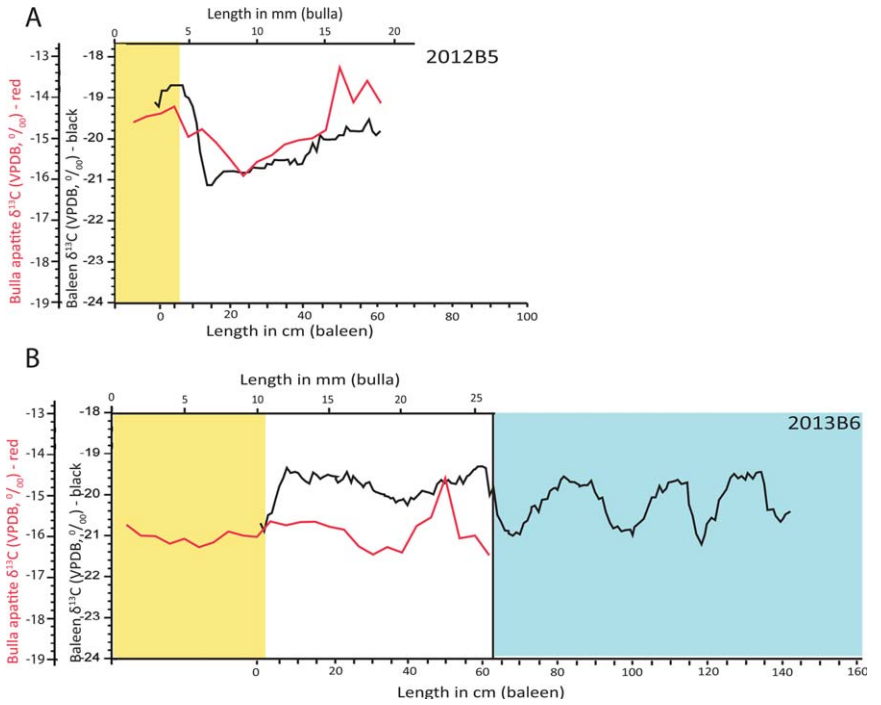

Figure 8. $\delta^{13}C$ values of bone apatite (red line) and baleen keratin (black line). Bone samples were taken along a transect of an involucrum slice from the center of region 1 of the involucrum (left) to the border between regions 1 and 2 (right). Baleen samples were taken along a transect the total length of the plate from distal (left) to proximal (right). Yellow area marks prenatally formed tissue, white indicates the nursing period, blue indicates the postweaning period. (A) NSB-DWM 2012B5. (B) NSB-DWM 2013B6.

(Marmontel *et al*. 1996) and other mysticetes (Klevezal 1996). This indicates that much of the structure of bowhead tympanic has remained unchanged since it was formed, and thus can form a record of the life of the individual. Our data indicate that the three morphological regions that we identified were formed during different parts of the life history of the animal.

Region 1 of the involucrum is deposited during the fetal period, as evidenced by NSB-DWM 2014B6F (Fig. 1C), a fetal specimen in which only region 1 of the tympanic is present. Fertilization in bowheads occurs around March (George *et al*. 2016), and this whale was caught in early October, hence region 1 represents approximately 6–7 mo of bone formation. Interestingly, baleen formation begins only a few months before birth (Thewissen *et al*. 2017), and none was present in this specimen when its mother was caught. Therefore, the isotopic record of the bone in region 1 of the involucrum represents a longer period of fetal life than the baleen plate does (Fig. 8). The border of the yellow and white area in Figure 8, marks the position where the neonatal notch was located on the baleen plate.

Region 2 of the bulla is deposited during the nursing period. This is evidenced by specimen NSB-DWM 2012B5 which displays only regions 1 and 2 (Fig. 1D, 2B), and is approximately 1 yr old based on the baleen length. Bowheads nurse for

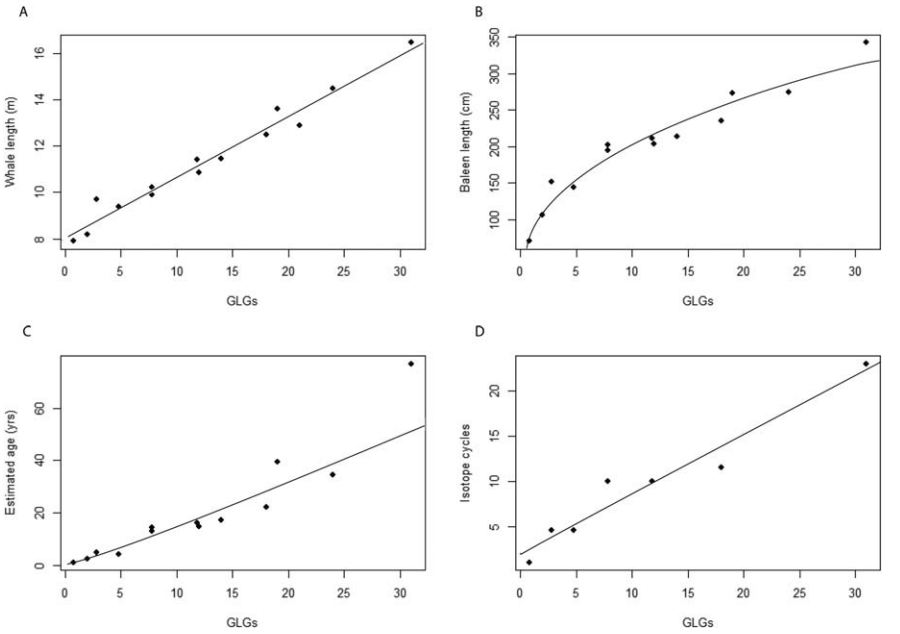

Figure 9. Tympanic bulla GLG counts plotted against four other variables from these same bowhead individuals. (A) Whale length (m) fitted to a linear regression line. (B) Longest baleen plate length (cm) fitted to a log-log regression curve. (C) Age estimated based on longest baleen plate (for model used, see text) fitted to a log-log regression. (D) Number of $\delta^{13}C$ isotope cycles in the longest baleen plate fitted to a linear regression line.

approximately 9 mo (George *et al*. 2016), and consistent with this, baleen of this individual displays only a single isotopic oscillation (Fig. 2A, Table 2). The isotopic signal ends when the whale was caught in the Chukchi Sea, likely around weaning. The seasonal oscillations that are evident in the isotope record of the baleen of independently feeding individuals (Schell *et al*. 1989*a, b*) are dampened in nursing whales due to the buffering effect of the mother's milk, the carbon and nitrogen of which are sourced from diet and body tissue stores (Newsome *et al*. 2010). This effect also occurs in isotope records of dentin in belugas (Matthews and Ferguson 2015*a*). We interpret the drop in $\delta^{15}N$ values of baleen as the end of nursing, and this occurs when the plate is between 62 and 92 cm long in our specimens (Fig. 2; NSB-DWM 2013B6, 2013B15, and 2015B19; nursing period with white background, independent feeding in blue).

Figure 8 shows the calibration of isotope records for baleen and regions 1 and 2 of the tympanic bone. The neonatal notch is calibrated to the end of region 1 (mentioned above) and the drop in isotope values of baleen is calibrated to the end of region 2. When both bone and baleen signals end suddenly these are calibrated because this is when the whale was harvested (Fig. 8A). Bone of the tympanic bulla does not grow at the same rate as baleen, but both record specific points in the life history of bowheads. The $\delta^{13}C$ values recorded from bone mineral of regions 1 and 2 of the tympanic bulla of NSB-DWM 2012B5 match those of its baleen, but this is not the case in 2013B6 (Fig. 8). The reason for this is unclear.

Table 2. List of bowhead whale specimens used, with some parameters studied and inferred results.

Whale ID	Season	Sex	Whale length (m)	Longest baleen (cm)	Age based on longest baleen length	Number of tympanic GLGs	Age based on baleen stable isotope cycles	Neonatal notch present
2011B9	Fall	F	12.5	235	22.2	18	11.5	no
2012B5	Spring	F	7.9	70.5	1.09	0.5	1	yes
2013B1	Fall	F	16.46	342	76.8	31	18	no
2013B5	Fall	M	9.9	195	12.8	7.5	10	no
2013B6	Fall	F	9.4	144	4.1	4.5	4.5	yes
2013B15	Fall	M	9.7	152	4.8	2.5	4.5	no
2013B18	Fall	F	11.4	211	16.2	11.5	10	no
2014B6F	Fall	—	—	none	—	none	none	fetus
2014B11	Fall	M	13.6	273	39.5	19		no
2014B14	Fall	F	10.2	202	14.3	7.5		no
2015B2	Spring	M	12.9			21		no
2015B16	Fall	M	10.87	204	14.8	12		no
2015B17	Fall	M	11.45	214	17.3	14		no
2015 B19	Fall	M	8.2	106	2.2	2	2	no
2015 B24	Fall	F	14.5	274	34.5	24		no

Region 3 of the tympanic is only found in whales older than 1 yr, and it represents slow periosteal growth with GLGs. This pattern has also been observed in the tympanic bone of fin (*Balaenoptera physalus)*, minke (*Balaenoptera acutorostrata*), and gray (*Eschrichtius robustus*) whales (Klevezal and Mitchell 1971; Christensen 1981, 1995; Klevezal *et al*. 1986; Klevezal 1996). The physiological reason why GLGs form is unclear, but the process has been studied in a variety of non-cetacean mammals. Köhler *et al*. (2012) showed that, in some ruminant species, formation of incremental growth layers is the result of cyclical endocrine and physiological changes that are related to the energetically unfavorable season. When feeding is limited, incremental growth layers are thinner. Huttenlocker *et al*. (2013) indicated that thick incremental growth layers reflect a period of robust growth, whereas thin ones indicate slow or ceased growth.

Castanet *et al*. (2004) proposed a different mechanism for GLG formation in the bones of the small arboreal primate *Microcebus*, showing conclusively that GLG formation was dependent on photoperiod during the year. Physiological variables that affect GLG formation are also known to be affected by photoperiod in arctic and subarctic artiodactyls, although these may be modulated by other environmental factors (Suttie and Webster 1995, Pösö 2003, Piccione *et al*. 2009).

Bowheads go through periods of robust feeding during summer in the Beaufort and Chukchi Seas and opportunistic and limited feeding during winter in the Bering Sea (George 2009). Thicker, dark colored incremental growth layers would be formed in summer, and thinner, light-colored layers in winter. Christensen (1981) came to similar conclusions for minke whale bullae based on results from teeth of seals and odontocetes. Thus, bowhead GLGs would be formed by a process that reflects seasonality and this process is probably not tightly tied to photoperiod, unlike *Microcebus*. This should not be a surprise given that the longest continuous light period in the Beaufort Sea lasts for more than 2 mo, and that winters in the Bering Sea have nights that last more than 21 h.

To assess the validity of GLG counts in bowhead tympanics as a means of age estimation, we regressed body length, baleen length, and age estimates based on baleen length against the number of GLGs (Fig. 9A–D). Overall, the correlation between body length and GLG numbers is strong and linear (Fig. 9A), but bowhead body length has been shown to plateau after weaning for much of the middle of the first decade of life (George *et al*. 2016), and this signal is not seen in our data. It is possible that a subtle growth trend is not recovered due to our small sample size, but other explanations are also possible. For instance, limited body growth and limited tympanic bone growth may co-occur. An extended period of low resource intake, such as the growth hiatus experienced in young bowheads, may result in a loss of annual resolution of growth patterns in the tympanic for that time in some individuals.

Baleen plate length increases with age, but the increment of annual growth slows (Fig. 9B) (Schell and Saupe 1993, Lubetkin *et al*. 2008, 2012, George *et al*. 2016), and a power function models the relation between GLG counts and baleen length reasonably well (Fig. 9B). Lubetkin *et al*. (2012) designed a model for relating baleen length to age (*y*-axis in Fig. 9C), and the outcome of this function correlates relatively closely to GLG counts, where the slope of 1 is evidence that one GLG accumulates each year. Indeed, age estimates based on the Lubetkin *et al*. (2012) model are similar to those of GLG counts (Table 2) in most individuals. A substantial difference occurs in NSB-DWM 2013B5 and 2014B14, where the Lubetkin *et al*. (2012) model predicts ages approximately twice that of the number of GLGs. We hypothesize that these two whales experienced some lean years with absence of GLG formation, or with GLGs so thin that they cannot be recognized.

Figure 9D shows that a positive linear relationship between baleen isotope oscillations and GLGs exists, however, the data are limited and the estimated slope differs from 1. This is partly caused by wear of the baleen, where entire annual migration records are lost in older whales. But the match between tympanic GLG numbers and isotope cycles is also not perfect for young individuals either. Here, it appears, again, that particulars of an individual's life history matter. Animals may be born in different seas, may migrate at different times, may wean earlier or later, and may spend more or less time in isotopically different areas of their range (Moore and Reeves 1993, Citta *et al*. 2015). For instance, NSB-DWM 2013B15 (Fig. 2E) shows two poorly resolved tympanic GLGs. These do not match the number of baleen isotopic oscillations which suggests 2 yr of independent feeding, plus 1 yr of nursing. The absence of clear GLGs may suggest that this whale did not experience the normal physiological stress that underlies the deposition of a thin incremental growth layer. Overall, Figure 9 indicates that GLGs provide reasonable estimates for age of individual whales, although they are not absolute and infallible age gauges.

Deposition of recognizable GLGs is influenced by unique events in the lives of bowhead individuals, and for older whales, GLGs become thin and indistinguishable from one another (Fig. 7B). This limits the use of GLGs for estimating age to younger individuals. A farther complication in distinguishing GLGs is that they do not form homogenously along the periosteal edge of the involucrum (Sukhovskaya *et al*. 1985, Klevezal 1996), and may become diffuse in some areas (Fig. 7A). Nonuniformity could be due in part to bone remodeling (arrowheads in Fig. 7B). Another issue is the distinction between GLGs and accessory layers (white boxes in Fig. 2D, 3B, 5A, 6C–E; Hohn 2009). Discussed by Larsen and Kapel (1982) and Olsen (2002), such accessory layers also occur in other tissues, such as teeth. Accessory layers may record particular transitory but important events in the life of the animal (Klevezal 1996, Hohn 2009), and mimic or overprint cyclical, annual patterns.

Conclusions

Tympanic GLGs can be used to estimate the age of bowhead whales, and we believe that this method is reliable up to ages of approximately 20 yr, somewhat reliable for ages between 20 and 30, but not reliable for older bowhead whales. This is broadly consistent with findings on the efficacy of this method in balaenopterid whales. As such, GLG counts are a useful addition to age estimation methods already available for bowheads. They hold particular promise for estimating the age of specimens where only limited samples are available, such as fossils or stranded specimens.

More important in our view is that tympanic GLGs are a window into the life history of the individual, and that histology of the tympanic bone records events that are not recorded in other anatomical samples. The recognition that region 1 and 2 of the tympanic are formed, respectively, in the fetal and nursing period, is an example thereof. Other life history parameters that could affect GLGs are feeding and migration. Thus, the GLGs in the tympanic of bowhead whales are more similar to a diary than to a calendar recording the individual's life.

ACKNOWLEDGMENTS

The authors would like to thank the hunters and residents of Barrow Alaska for allowing sampling of the whales and for their trust and support. This project benefitted from the assistance of the North Slope Borough, Department of Wildlife Management (NSB-DWM) and

in particular Taqulik Hepa, Janell Kaleak, Molly Spicer, Lucia Johnston, Malissa Langley, Bobby Sarren, and Dave Ramey. We thank Mary Nerini for her pioneering work on growth lines in the tympanic of Alaskan bowhead whales. We also thank Shanna McCleary and Tyler Kerr at the University of Wyoming for their assistance in sample processing. Funding and support for this project came from the North-Slope Borough (NSB), Kent State University School of Biomedical Science, NEOMED, and the NSB-Shell Baseline Studies Program.

Literature Cited

Castanet, J., S. Croci, F. Aujard, M. Perret, J. Cubo and E. De Margerie. 2004. Lines of arrested growth in bone and age estimation in a small primate: *Microcebus murinus*. Journal of Zoology London 263:31–39.

Christensen, I. 1981. Age determination of minke whales, *Balaenoptera acutorostrata*, from laminated structures in the tympanic bullae. Report of the International Whaling Commission 31:245–253.

Christensen, I. 1995. Interpretation of growth layers in the periosteal zone of *tympanic bulla* from minke whales *Balaenoptera acutorostrata*. Pages 413–425 *in* A. S. Blinx, L. Walløe and Ø. Ulltang, eds. Whales, seals, fish and man: Developments in marine biology. Elsevier Science B.V., Amsterdam, The Netherlands.

Citta, J. J., L. T. Quakenbush, S. R. Okkonen, *et al*. 2015. Ecological characteristics of core-use areas used by Bering-Chukchi-Beaufort (BCB) bowhead whales, 2006–2012. Progress in Oceanography 136:201–222.

Currey, J. D. 2003. The many adaptations of bone. Journal of Biomechanics 36:1487–1495.

De Ricqlès, A., J. Meunier, F. J. Castanet and H. Francillon-Vieillot. 1991. Comparative microstructure of bone. Pages 1–78 *in* B. K. Hall, ed. Bone volume 3: Bone matrix and bone specific products. CRC Press, Boca Raton, FL.

Francillon-Vieillot, H., V. De Buffrenil, J. Castanet, *et al*. 1990. Microstructure and mineralization of vertebrate skeletal tissues. Pages 471–548 *in* J. G. Carter, ed. Skeletal biomineralization: Patterns, processes and evolutionary trends. Van Nostrand Reinhold, New York, NY.

George, J., J. L. Bada, J. Zeh and R. Suydam. 1999. Age and growth estimates of bowhead whales (*Balaena mysticetus*) via aspartic acid racemization. Canadian Journal of Zoology 77:571–580.

George, J. C. 2009. Growth Morphology and energetics of bowhead whales (*Balaena mysticetus*). Ph.D. thesis, University of Alaska Fairbanks, Fairbanks, AK. 168 pp.

George, J. C., E. Follmann, J. Zeh, M. Sousa, R. Tarpley, R. Suydam and L. Horstmann-Dehn. 2011. A new way to estimate the age of bowhead whales (*Balaena mysticetus*) using ovarian corpora counts. Canadian Journal of Zoology 89:840–852.

George, J. C., R. Stimmelmayr, R. Suydam, S. Usip, G. Givens, T. Sformo and J. G. M. Thewissen. 2016. Severe bone loss as part of the life history strategy of bowhead whales. PLOS One 11:1–14.

Hobson, K. A., and D. M. Schell. 1998. Stable carbon and nitrogen isotope patterns in baleen from eastern Arctic bowhead whales (*Balaena mysticetus*). Canadian Journal of Fisheries and Aquatic Sciences 55:2601–2607.

Hohn, A. 2009. Age estimation. Pages 11–17 *in* W. F. Perrin, B. Würsig and J. G. M. Thewissen, eds. Encyclopedia of marine mammals. Academic Press, Amsterdam, The Netherlands.

Huttenlocker, A. K., H. N. Woodward and B. K. Hall. 2013. The biology of bone. Pages 13–34 *in* K. Padian and E.-T. Lamm, eds. Bone histology of fossil tetrapods: Advancing methods, analysis, and interpretation. University of California Press, Berkeley, CA.

Klevezal, G. A. 1996. Recording structures of mammals: Determination of age and reconstruction of life history. A.A. Balkema, Rotterdam, The Netherlands.

Klevezal, G. A., and E. D. Mitchell. 1971. Year layers in bones of whalebone whales. [In Russian with English summary.] Zoologicheskiĭ zhurnal 50:1114–1116.

Klevezal, G. A., L. I. Sukhovshaya and S. A. Blokhin. 1986. Age determination in baleen whales by annual layers in the bone. [In Russian with English summary.] Zoologicheskiĭ zhurnal 65:1722–1730.

Köhler, M., N. Marín-Moratalla, X. Jordana and R. Aanes. 2012. Seasonal bone growth and physiology in endotherms shed light on dinosaur physiology. Nature 487:358–361.

Konrádsson, A., and J. Sigurjónsson. 1989. Studies of growth layers in tympanic bullae of fin whales (*Balaenoptera physalus)* caught off Iceland. Report of the International Whaling Commission 39:277–279.

Larsen, F., and F. O. Kapel. 1982. Norwegian minke whaling off West Greenland 1967–80 and biological studies of West Greenland minke whales. Report of the International Whaling Commission 32:263–274.

Larsen, F., and F. O. Kapel. 1983. Further biological studies of the West Greenland minke whale. Report of the International Whaling Commission 33:329–332.

Lee, S. H., D. M. Schell, T. L. McDonald and W. J. Richardson. 2005. Regional and seasonal feeding by bowhead whales *Balaena mysticetus* as indicated by stable isotope ratios. Marine Ecology Progress Series 285:271–287.

Lubetkin, S. C., J. E. Zeh, C. Rosa and J. C. George. 2008. Age estimation for young bowhead whales (*Balaena mysticetus*) using annual baleen growth increments. Canadian Journal of Zoology 86:525–538.

Lubetkin, S. C., J. E. Zeh and J. C. George. 2012. Statistical modeling of baleen and body length at age in bowhead whales (*Balaena mysticetus*). Canadian Journal of Zoology 90: 915–931.

Marmontel, M., T. J. O'Shea, H. I. Kochman and S. R. Humphrey. 1996. Age determination in manatees using growth-layer-group counts in bone. Marine Mammal Science 12:54–88.

Matthews, C. J. D., and S. H. Ferguson. 2015*a*. Seasonal foraging behavior of Eastern Canada-West Greenland bowhead whales: An assessment of isotopic cycles along baleen. Marine Ecology Progress Series 522:269–286.

Matthews, C. J. D., and S. H. Ferguson. 2015*b*. Weaning age variation in beluga whales (*Delphinapterus leucas*). Journal of Mammalogy 96:425–437.

Moore, S. E., and R. R. Reeves. 1993. Pages 313–386 *in* J. J. Burns, J. J. Montague and C. J. Cowles, eds. The bowhead whale. Special Publication Number 2. The Society for Marine Mammalogy.

Newsome, S. D., M. T. Clementz and P. L. Koch. 2010. Using stable isotope biogeochemistry to study marine mammal ecology. Marine Mammal Science 26:509–572.

Olsen, E. 2002. Errors in age estimates of North Atlantic minke whales when counting growth zones in bulla tympanica. Journal of Cetacean Research and Management 4:185–191.

Olsen, E., N. Øien, A. Leithe and B. Bergfløt. 2003. The suitability of mandible growth layers in the common minke whale (*Balaenoptera acutorostrata*) for age determination. Journal of Cetacean Research and Management 5:93–101.

Perrin, W. F., and A. C. Myrick, Jr. 1980. Report of the workshop. Age determination of toothed whales and sirenians. Report of the International Whaling Commission (Special Issue 3):1–50.

Piccione, G., C. Giannetto, S. Casella and G. Caola. 2009. Annual rhythms of some physiological parameters in *Ovis aries* and *Capra hircus*. Biological Rhythm Research 40:455–464.

Pösö, R. A. 2003. Seasonal changes in reindeer physiology. Rangifer 25:31–38.

Rosa, C., J. C. George, J. Zeh, O. Botta, M. Zauscher, J. Bada and T. M. O'Hara. 2004. Update on age estimation of bowhead whales (*Balaena mysticetus*) using aspartic acid racemization. International Whaling Commission SC/56/BRG6:1–15.

Saupe, S. M., D. M. Schell and W. B. Griffiths. 1989. Carbon-isotope ratio gradients in Western Arctic zooplankton. Marine Biology 103:427–432.

Schell, D. M. 1992. Stable isotope analysis of 1987–1991 zooplankton samples and bowhead whale tissues. Report to U.S. Minerals Managements Service OCS Study MMS 92-0020. 101 pp.

Schell, D. M., and S. M. Saupe. 1993. Feeding and growth as indicated by stable isotopes. Pages 491–509 *in* J. J. Burns, J. J. Montague and C. J. Cowles, eds. The bowhead whale. Special Publication Number 2. The Society for Marine Mammalogy.

Schell, D. M., S. M. Saupe and N. Haubenstock. 1989*a*. Bowhead whale (*Balaena mysticetus*) growth and feeding as estimated by $\delta^{13}C$ techniques. Marine Biology 103:433–443.

Schell, D. M., S. M. Saupe and N. Haubenstock. 1989*b*. Natural isotope abundances in bowhead whale (*Balaena mysticetus*) baleen: Markers of aging and habitat usage. Pages 260–269 *in* P. W. Rundel, J. R. Ehleringer and K. A. Nagy, eds. Stable isotopes in ecological research. Springer, New York, NY.

Sukhovskaya, L. I., G. A. Klevezal, V. I. Borisov and S. J. Lagerev. 1985. Use of bone layers to determine age in minke whales. Acta Theriologica 30:275–285.

Suttie, J. M., and J. R. Webster. 1995. Extreme seasonal growth in arctic deer: Comparisons and control mechanisms. American Zoologist 35:215–221.

Suydam, R. S., and J. C. George. 2004. Subsistence harvest of bowhead whales (*Balaena mysticetus*) by Alaskan Eskimos, 1974–2003. The International Whaling Commission SC/56/BRG12:1–12.

Tarpley, R. J., D. J. Hillmann, J. C. George, J. E. Zeh and R. S. Suydam. 2016. Morphometrics correlates of the ovary and ovulatory corpora in the bowhead whale, *Balaena mysticetus*. The Anatomical Record 299:769–797.

Thewissen, J. G. M., T. L. Hieronymus, J. C. George, R. Suydam, R. Stimmelmayr and D. McBurney. 2017. Evolutionary aspects of the development of teeth and baleen in the bowhead whale. Journal of Anatomy 230:549–566.

Withrow, D., R. Burke, Jr., L. Jones and J. Brooks. 1992. Variations in $\delta^{13}C$ carbon isotope ratios in bowhead whale baleen plates used to estimate age. Report of the International Whaling Commission 42:469–473.

Woodward, H. N., K. Padian and A. H. Lee. 2013. Skeletochronology. Pages 195–215 *in* K. Padian and E.-T. Lamm eds. Bone histology of fossil tetrapods: Advancing methods, analysis, and interpretation. University of California Press, Berkeley, CA.

Zenitani, R., and H. Kato. 2010. The growth of baleen plates in Antarctic minke whales, with special reference to the V-shape notch appearing at the outer edge of the plates. Nippon Suisan Gakkaishi 76:870–876.

Received: 29 August 2016
Accepted: 17 September 2017